

## **Graphene oxide improves the biocompatibility of collagen membranes in an *in vitro* model of human primary gingival fibroblasts**

Patrizia De Marco,<sup>a</sup> Susi Zara,<sup>a</sup> Marianna De Colli,<sup>a</sup> Milena Radunovic,<sup>b</sup> Vladimir Lazović,<sup>c</sup> Valeria Ettore,<sup>a</sup> Antonello Di Crescenzo,<sup>a</sup> Adriano Piattelli,<sup>d</sup> Amelia Cataldi,\*<sup>a</sup> Antonella Fontana\*<sup>a</sup>

<sup>a</sup> Department of Pharmacy, Università “G. d’Annunzio”, Via dei Vestini, 66100 Chieti, Italy

<sup>b</sup> School of Dental Medicine, University of Belgrade, 11000, Belgrade, Serbia

<sup>c</sup> Institute of Physics, University of Belgrade, 11080 Zemun, Belgrade, Serbia

<sup>d</sup> Department of Medical, Oral and Biotechnological Sciences, Università “G. d’Annunzio”, Via dei Vestini, 66100 Chieti, Italy

### **Abstract**

Commercial collagen membranes are used in oral surgical procedures as scaffolds for bone deposition in guided bone regeneration. Here, we have enriched them with graphene oxide (GO) via a simple non-covalent functionalization and exploiting the capacity of oxygenated carbon functional moieties of GO to interact through hydrogen bonding with collagen. In the present paper, the GO-coated membranes have been characterized in terms of stability, nano-roughness, biocompatibility and induction of inflammatory response towards *HGFs* cells. The obtained coated membranes demonstrate to not leak GO in the bulk solution and to change some features of the membrane, such as stiffness and adhesion of the membrane for the AFM tip. Moreover, the presence of GO increases the roughness and the total surface exposed to the cells as demonstrated

by AFM analyses. The obtained material is biocompatible and does not induce inflammation in the tested cells.

## **Introduction**

Barrier membranes are standardly used in oral surgical procedures exploiting guided tissue regeneration (GTR) and guided bone regeneration (GBR) for the treatment of periodontal bone defects and peri-implant defects, as well as for bone augmentation [1,2]. The aim is to place the membrane in order to prevent the ingrowth of soft connective tissue into bone defects, and therefore create a secluded space into which only cells from the neighboring bone can migrate [3]. The muco-periosteal flap is then repositioned over the membrane and sutured. The membranes can be made of non-resorbable materials, such as expanded polytetrafluoroethylene (ePTFE), or resorbable materials, such as synthetic polyesters (polyglycolides, polylactides, or copolymers thereof) or collagen. In addition, resorbable membranes don't need a second intervention to be removed once bone has been reformed, thus decreasing the risk of infection and the loss of some of the regenerated bone. Last but not least, the lack of a second intervention is desirable and cost-effective for the patient. Collagen membranes disclose several advantages, compared to polymeric membranes, such as easy manipulation, weak immunogenicity [4], a direct effect on bone formation and chemotaxis of gingival and periodontal ligament fibroblasts [5,6]. The source of the collagen is various, but typically it is obtained from bovine tendon, bovine dermis, calf skin, or porcine dermis [1]. In the attempt to improve the biocompatibility and promote the desired effect on the surrounding tissues, a lot of collagen membranes modifications were proposed. Such modifications included cross-linking [7], the addition of heparan sulfate and fibronectin [8] or nanobioactive glass [9]. Here, we plan to improve the properties of collagen membranes by coating them with graphene oxide (GO).

Indeed, graphene is a flat monolayer of carbon atoms tightly packed into a two-dimensional (2D) honeycomb lattice and is a basic building block for graphitic materials with unique physical, chemical, and mechanical properties [10]. In particular, graphene oxide, an oxidized derivative of graphene, was so far actively investigated in the biomedical field, due to its solubility in water and its reactive oxygen functional groups [11], that make it a good candidate for enzyme adsorption [12], cell imaging and drug delivery [13,14]. However, in order to use GO as a biomaterial, its biosafety and biocompatibility has to be confirmed in both cell cultures and live biosystems. Many reports show that GO is a biocompatible material that discloses limited or no cytotoxicity, and allow the effective proliferation of human and mammalian cells. In fact, several reports showed that, when grown on GO paper, the adhesion and proliferation of different cells, such as L-929 cells [15], osteoblasts [16,17], kidney cells, and embryonic cells [18] is promoted. In particular, Ferrari et al. report that no cytotoxicity effects are evidenced when graphene is used as support for tissue regeneration or cell growth suggesting that graphene is safe if remains intact after cell growth [19]. These combined results support that GO materials are biocompatible and rather promote cell adhesion and proliferation. In particular, the dose-dependent cytotoxicity of GO is evident when cells are exposed to colloidal solutions of GO [20,21], whereas is minimal when GO flakes are used to cover different biomaterials [22].

The aim of this study was therefore to prepare collagen membranes enriched with GO. In particular, we were able to optimize the coating protocol, chemico-physically characterize the obtained coated membranes and ascertain that the coating was stable and did not leak graphene oxide in the bulk medium. A relevant section of the paper is devoted to the superficial characterization of the coated membrane by using atomic force microscopy. The following step was to investigate the biocompatibility of the obtained enriched collagen membranes with human

primary gingival fibroblasts (HGFs), which are the first cells adhering to the membrane during healing. In particular, we evaluated the viability and metabolic activity as well as the cytotoxic and the inflammatory response of HGFs grown on collagen membranes coated with two concentrations of GO, 2 and 10  $\mu\text{g/ml}$ . These two concentrations were chosen by considering that GO coated porcine bone granules performed by using concentration of 50  $\mu\text{g/ml}$  [22] demonstrated to release in the surrounding tissue an appreciable amount of not perfectly adsorbed GO.

## **Methods**

### *Materials*

Synthetic Graphite  $\sim$  200 mesh, 99.9995% powder was purchased from Alfa Aesar. Collagen membranes (Osteobiol Derma®, TecnoSS), derived from porcine dermis after removal of the epithelial layer, were a gift of TecnoSS Dental s.r.l. Pianezza (TO), Italy.

### *Preparation of graphene oxide*

Graphene oxide (GO) was prepared by slightly modifying the Hummers method [23,24]. A flask containing 0.2 g of graphite and 0.1 g of sodium nitrate in 4.6 ml of concentrated sulfuric acid was placed in an ice bath. The mixture was added of 0.6 g potassium permanganate under continuous stirring. After 2 h, the reaction mixture was transferred in a water bath at 35 °C and stirred for 30 min. Deionized water (9.2 ml) was slowly added to the solution and the flask was heated to 98°C for 45 min. 27.8 ml of deionized water and 2.14 ml of 30% hydrogen peroxide were poured in the mixture to stop the reaction. The obtained light brown mixture was filtered through a sintered-glass filter (pore size 15-40  $\mu\text{m}$ ) and rinsed three times with 5% HCl and then with deionized water. The solid was dried in oven at 60°C for 12 h. The obtained graphite oxide was redispersed in water, ultrasonicated for 45 min and centrifuged for 15 min at 9000 rpm. Rotary evaporation at 40 °C of the corresponding supernatant allowed to obtain exfoliated graphene oxide, GO. The

obtained GO quality was assessed by using spectrophotometry, FTIR and Raman spectroscopies, Dynamic Light Scattering,  $\zeta$ -potential, TEM and SEM techniques [22].

#### *Enrichment of collagen membranes*

Different GO aqueous solutions were prepared by ultrasonating the proper amount of GO in water for 30 min and subsequently centrifugating the suspension at 5500 rpm for 15 min. The GO concentration in water was adjusted in order to obtain two diluted solution, namely 2 and 10  $\mu\text{g/ml}$ . Then, the membranes (20 $\times$ 30 mm lateral dimensions) were cut with a cutter to obtain square pieces of membrane (5 $\times$ 5 mm lateral dimensions). Half of such samples were covered with 100  $\mu\text{l}$  of the 2  $\mu\text{g/ml}$  GO solution, while the other half was covered with 100  $\mu\text{l}$  of the 10  $\mu\text{g/ml}$  GO solution. The liquid was left to evaporate overnight under fumehood. The rinsed pieces (see Figure 1) were transferred in a 96 multiwell plate for the biocompatibility tests. We chose to cut the membranes in small pieces before wetting them with the GO solution in order to avoid the edge rippling of the membrane during the dry process and to have a more uniform distribution of the GO sheets on the surface and in the core of the membrane.

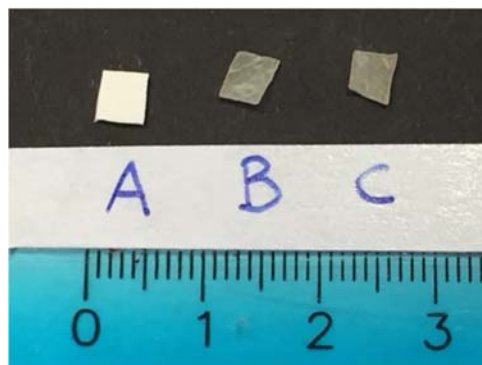


**Figure 1** Photograph of bare membrane (A), 2  $\mu\text{g/ml}$  GO-enriched membrane (B) and ), 10  $\mu\text{g/ml}$  GO-enriched membrane (C).

#### *Characterization of the GO-enriched material*

The obtained GO-enriched membranes were characterized by using Multimode 8 Bruker AXS SAS Atomic Force microscopy (AFM) and Scanning Electron Microscopy (SEM) analyses. AFM measurements were performed using a Digital Multimode 8 Bruker AFM microscope with Nanoscope V controller and using commercial silicon tips (cantilever resonance frequency of 75 kHz and nominal elastic constant of 3 N/m) with a typical apex radius of 10 nm. In order to perform quantitative nanomechanical investigations of height, deformation, dissipation energy and adhesion at each point across  $1\ \mu\text{m} \times 1\ \mu\text{m}$  sized area of the prepared samples, the Peak Force QNM mode with ScanAsyst™ in air was used. The deflection sensitivity and tip radius were calibrated for each probe prior to use, against standard sapphire. AFM images were analyzed with the WSxM software [25].

Stability measurements were performed by using a Cary 100 bio Varian spectrophotometer. Samples were investigated by scanning electron microscopy using high resolution electron microscope MIRA3 FEG-SEM, Tescan at accelerating voltage 20 kV. Before that, the surface of samples was coated with an ultrathin gold layer using SC7620 Mini Sputter Coater, Quorum Technologies, with the purpose to prevent the accumulation of static electric fields at the specimen due to the electron irradiation required during imaging.

#### *Isolation and culture of HGFs*

Donors subjected to the extraction of the third molar signed informed consent, according to Italian Legislation and with the code of Ethical Principles for Medical Research involving Human Subjects of the World Medical Association (Declaration of Helsinki). The project obtained the approval of Local Ethical Committee of the University of Chieti (approval number 1173, date of approval 31/03/2016). Donors, aged from 20 to 40 years, were not affected by any systemic conditions, didn't take medication and tobacco. Gingival fragments were obtained from the

retromolar area as a consequence of the surgical flap regularization before suture. Fragments of healthy gingival tissue were immediately placed in Dulbecco's modified Eagle's medium DMEM (Euroclone, Pero, MI, Italy) for at least 1 h, rinsed three times in phosphate buffered saline solution (PBS), minced into small tissue pieces and cultured in DMEM containing 10% fetal bovine serum (FBS) and antibiotics (1% penicillin and streptomycin), 1% fungizone (all purchased from Euroclone, Pero, MI, Italy). After one week, fungizone was removed from culture medium and the gingival fragments were cultured until HGFs appear (at least 3 weeks). All cells were maintained at 37 °C in a humidified atmosphere of 5% (v/v) CO<sub>2</sub>. Cells were processed after 4-8 passages. All the experiments were realized with cells obtained from two different donors and each assay was performed in triplicate. 24 hours before cell seeding, membranes were immersed in medium. HGFs were seeded at  $7.5 \times 10^3/\text{cm}^2$  concentration in 48-well non-treated plates containing the membranes and cultured for 1, 3 and 7 days.

#### *Sterilization of membranes*

Both bare and GO-enriched membranes were UV irradiated (UV lamp 15 W) for 2h in order to sterilize the samples. The stability of the irradiated membranes was monitored via spectrophotometric measurements in analogy to measurements performed on non-irradiated membranes.

#### *Alamar blue cell viability assay*

For Alamar blue assay, 3 membranes for each experimental group at each time point were used. HGFs viability was evaluated after 1, 3 and 7 days of culture by Alamar blue assay based on the capability of viable cells to reduce Alamar blue reagent into a red product. At established time points the medium was replaced by a fresh one containing Alamar blue reagent (Thermo Scientific, Rockford, IL, USA) in 10% of the volume, probed with cells for 4 h at 37°C and read at 570 and

600 nm. Value obtained in the absence of cells was considered as negative control. The % reduction of Alamar blue reagent was calculated according to manufactured instruction.

#### *Cytotoxicity assay (LDH assay)*

To assess membrane integrity of HGFs, lactate dehydrogenase (LDH) leakage into the medium was quantified using “CytoTox 96 non-radioactive cytotoxicity assay” (Promega, Madison, WI, USA), as suggested by the manufacturer, after 1, 3 and 7 days of culture on the different experimental membranes. In each well, the LDH leakage measured in the supernatant was normalized to the total intracellular LDH value obtained after cell lysis.

#### *ELISA test of IL6 and PGE2 secretion*

IL6 and PGE2 secretion in the culture medium at the different experimental times for all samples was detected by following the instructions provided by the manufacturer. EIA kit (Enzo Life Sciences, Farmingdale, NY, USA) was used to determinate IL6 and PGE2 concentrations. Absorbance values were obtained by spectrophotometric reading at 450 and 405 nm, respectively, by means of Multiscan *GO* 96-well microplate spectrophotometer (Thermo Scientific, Rockford, IL, USA). Secretion levels of IL6 and PGE2 were measured in different wells and normalized for % Alamar blue reduction values, as previously determined by Alamar blue assay.

## **Results**

The enrichment with GO was visually detected by comparing the bare ~~pure~~ membrane with GO-coated membranes enriched with different concentrations of GO. Figure 1 shows membranes coated with 2 µg/ml and 10 µg/ml GO solutions. The UV irradiation used for the sterilization of the membranes did not change the color of the coating from brown to black (the color of reduced GO) [26] thus confirming that GO did not reduce under the experimental conditions adopted.



Indeed reduction of GO has been obtained by Han *et al.* by using a much higher lamp power (500 W) [27].

In most composite materials, an effective wetting and an uniform dispersion of components in a given matrix, as well as a strong interfacial adhesion between the coating and the underlying collagen-membrane, are required to obtain an enriched material with satisfactory mechanical and biocompatibility properties.

AFM analyses allowed us to obtain molecular imaging (Figure 2) as well as quantitative nano-mechanical mapping of the coated membranes. In Figure 2 the topographic map of the bare membrane and of the GO-coated membrane are displayed, showing the typical aspect of the pristine membrane in panel A, and that of the GO-covered material in panel B.

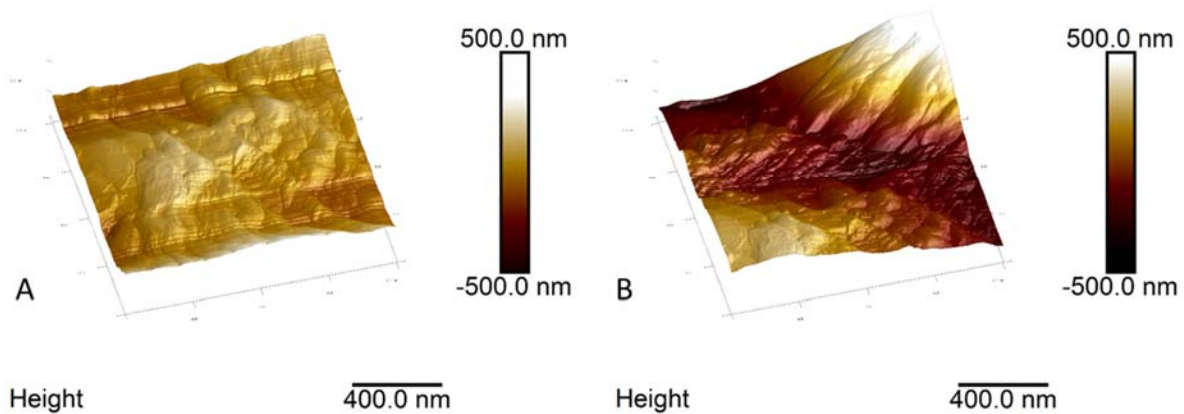


**Figure 2** AFM images of tridimensional topography of the collagen membrane (A) and the GO-enriched membrane (B).

Peak Force QNM provides images at a relatively high speed and a high resolution, quantifying the mechanical features of the sample (Figure S1-S11 in the Supplementary Data). Peak Force has been widely used to investigate the mechanical effects on biological samples [28,29]. Figure 3

reports the maps of peak force error (panels A and E), adhesion (panels B and F), dissipation (panels C and G) and deformation (panels D and H), respectively of bare collagen membrane (upper images) and 10  $\mu\text{g/ml}$  GO-coated membrane (lower images). The pure membrane (Figure 3, panel A) appears quite corrugated with a total thickness of at least 300 nm. In particular, the image evidences the presence of collagen fibers forming the membrane (see also Figure 4, panel A). Panel E of Figure 3 highlights the presence, in the upper right corner, of a different material, i.e. graphene oxide flake, that covers the membrane, rendering it different in terms of adhesion, dissipation and deformation.

The adhesion (panels B and F) is determined by comparing the adhesion force region between tip approach and retracing during the scanning surface of the sample. The obtained data highlight that the adhesion of the tip to the surface increases on coating the membrane with GO from  $1.9\pm 0.2$  nN (Figure S1 of the Supplementary Data) to  $2.3\pm 0.9$  nN (Figure S2 of the Supplementary Data), with values of  $2.4\pm 1.2$  onto the GO flake and  $1.3\pm 0.6$  in the bottom region of the coated membrane (Figures S3 and S4 of the Supplementary Data).

Panel C shows that the dissipation energy for the bare membrane ranges from 0.1 to 1 keV with a mean value of  $120\pm 30$  eV (Figure S5 of the Supplementary Data). The dissipation energy measures the hysteresis between the loading and unloading curves of the cantilever and therefore can give information on the elastic behavior of the sample, being elastic samples characterized by low dissipation energy values. In the present case the obtained dissipation energy is indicative of a non perfectly elastic sample (i.e. viscoelastic behavior). In the presence of GO (Panel G) the dissipation energy map splits the sample in two well defined regions: the top right region, with the recognizable GO flake, in which the dissipation energy increases to  $160\pm 20$  eV (Figure S6 of the

Supplementary Data), and the lower region that keeps a relatively lower value of  $150 \pm 10$  eV (Figure S7 of the Supplementary Data).

Panels D and H report the deformation data, i.e. the degree of indentation of the tip into the surface at the peak force. The bare membrane has a mean deformation of  $1.9 \pm 0.6$  nm (Figure S8 of the Supplementary Data) whereas the coated membrane has a lower mean deformation of  $1.4 \pm 0.9$  nm (Figure S9 of the Supplementary Data), with values of  $1.4 \pm 0.8$  nm and  $0.9 \pm 0.2$  nm for the GO flake region (upper right corner) and the bottom region, respectively (See Figures S10 and S11 of the Supplementary Data).

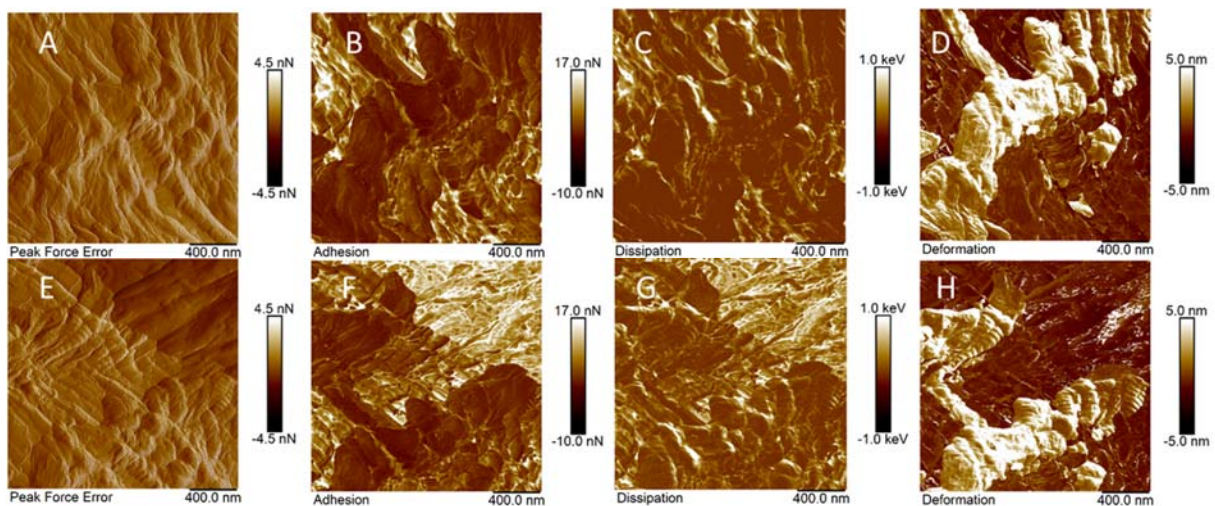


**Figure 3** AFM images of bare membrane (upper images) and 10  $\mu\text{g/ml}$  GO-enriched membrane (lower images). Panels A and E report peak force error; panels B and F report adhesion; panels C and G report dissipation and panels D and H report deformation. Scale bar is 400 nm in all cases.

Nano-roughness evaluation was performed on the same instrument in Peak Force QNM operation mode (see Figure S12 and 13 in the Supplementary Data).

Stability measurements (Figure 4) were performed by keeping the membrane in contact with water under static or shaken conditions, before and after UV irradiation. The absorbance at 230 nm, the  $\lambda_{\text{max}}$  of GO, of the bulk aqueous solution was checked after 1, 3 and 7 days. No evidence of graphene oxide dissolution was observed being the absorbance of the bulk solution comparable with that recovered from the blank (a non-coated membrane). The increase of absorbance observed on passing from 1 to 7 days of immersion in the bulk solution is probably due to dissolution of collagen. As a matter of fact the collagen membrane showed an absorbance spectrum in the 200-350 nm wavelength interval with a shoulder at 250 nm. It is interesting to note that irradiation reduced the collagen solubility in the bare membrane due to effective irradiation induced-crosslinking of collagen and subsequent reduction of solubility [30].

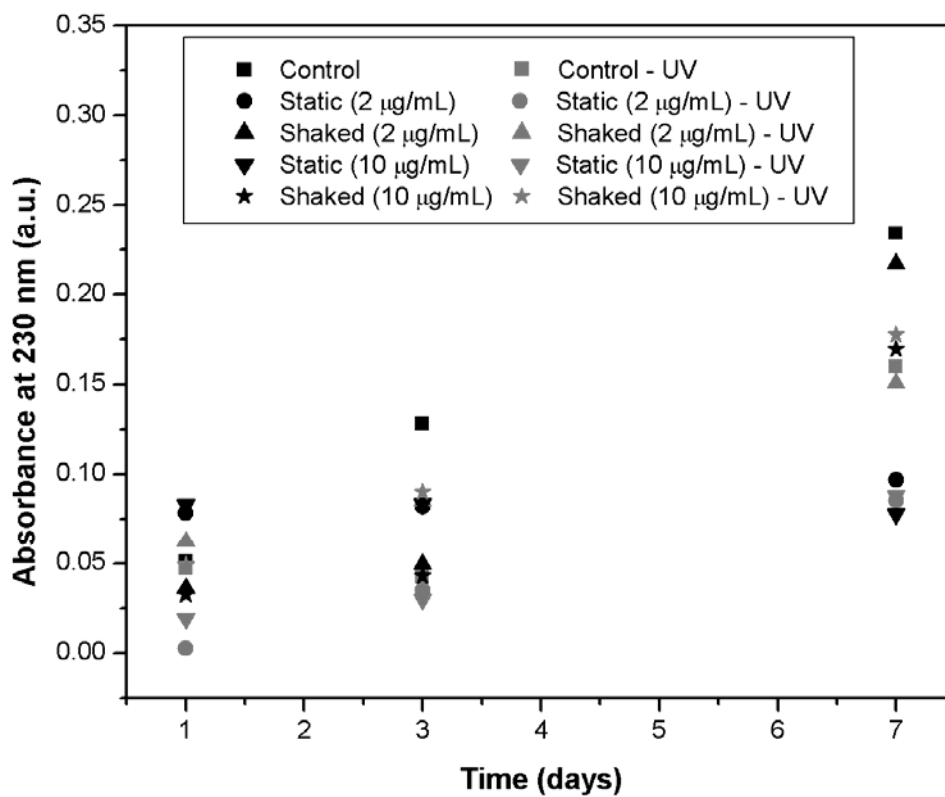


**Figure 4** Stability measurements of GO coated (2 and 10  $\mu\text{g/ml}$ ) and uncoated (blank) membranes. The membranes were immersed in milliQ water under static or shaken conditions and before and after UV irradiation. The absorbance of the bulk solution was measured at 1, 3 and 7 days.

SEM analyses (Figure 5) demonstrated, as well, the ability of graphene oxide to coat the membrane, although the lack of the network of collagen fibers in the coated samples is mainly due to the preparation protocol that implies a simple air drying of the samples rather than to a real GO-coating. As a matter of fact, SEM is not the elected method for the evaluation of the homogeneity of the GO-coating. In order to obtain such a detailed visualization of collagen fibers, the coated samples should have been thoroughly dehydrated by performing several rinses with ethanol or heating at high temperatures, but both these processes could have altered the features of the final membrane.

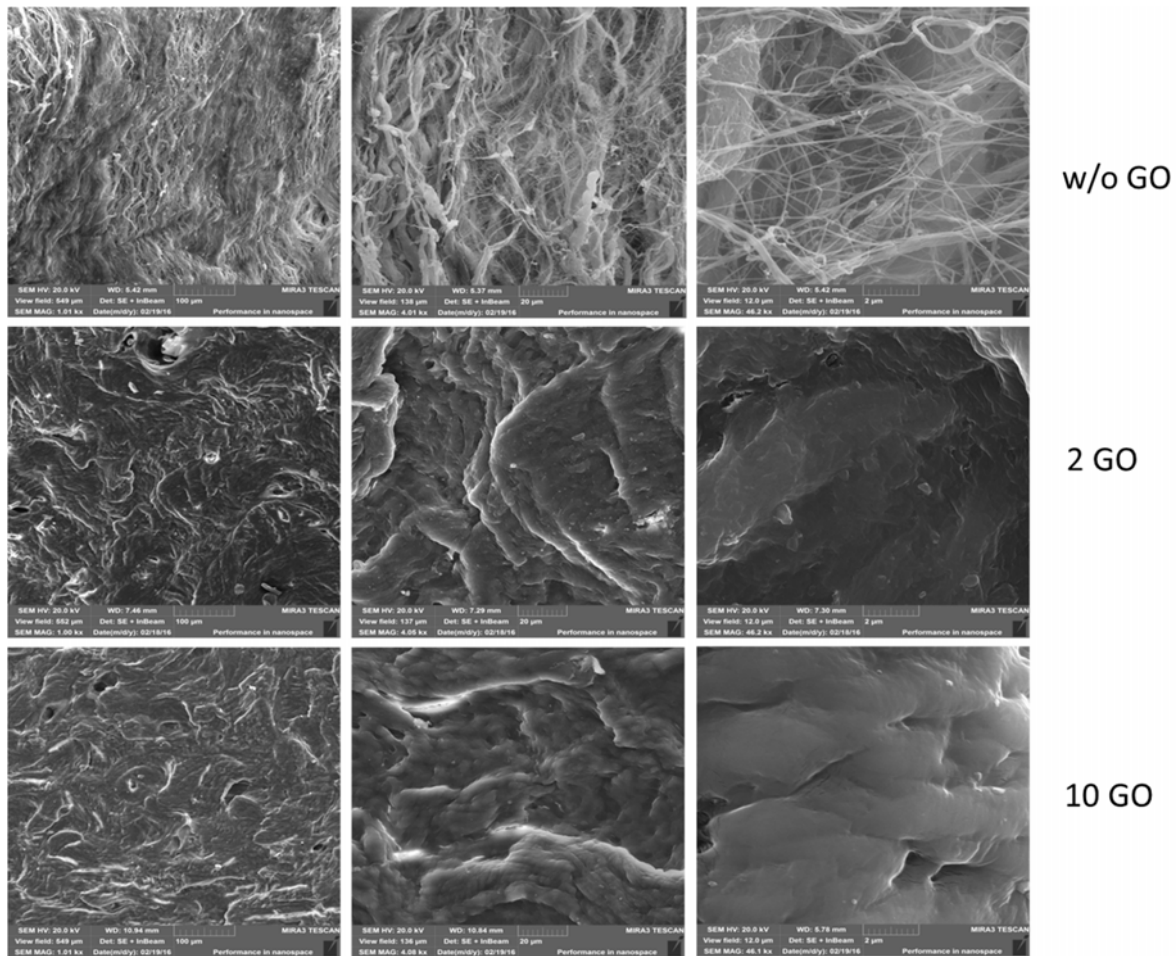


**Figure 5** SEM images of bare and completely dehydrated membranes (upper images), 2 µg/ml GO-enriched membrane (central images) and 10 µg/ml GO-enriched membrane (lower images). Panels on the left report a magnification of 1.01 k, central panels a magnification of 4.05 k and right panels a magnification of 46.1 k. Scale bar are consequently 100 µm, 20 µm and 12 µm from left to right.

*HGFs* were cultured on uncoated collagen membranes (control) and on 2 µg/ml GO and 10 µg/ml GO-coated collagen membranes for 1, 3 and 7 days. All the assays were performed at the three established experimental times.

Alamar blue assay, performed in order to measure the cell metabolic activity, showed an expected increase over time due to cellular proliferation. At day 3 the metabolic activity of the cells grown on membrane coated with both 2  $\mu\text{g/ml}$  GO and 10  $\mu\text{g/ml}$  GO was significantly higher than that monitored on the control membrane, whereas no significant difference was recorded at other experimental times (Figure 6).

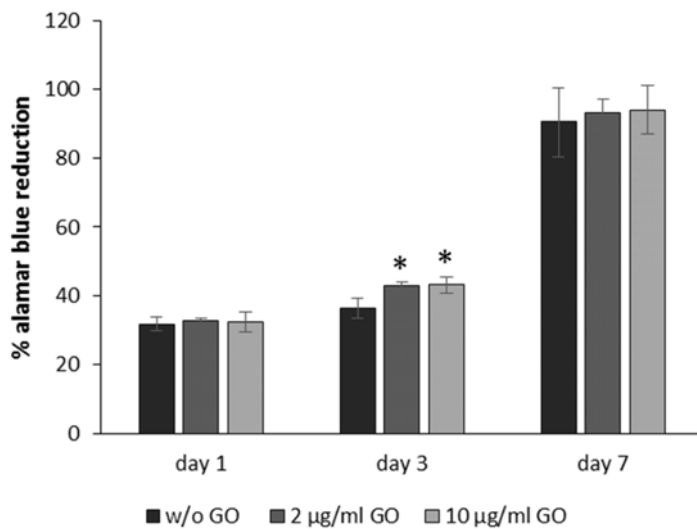


**Figure 6** Alamar blue assay in *HGFs* cultured on uncoated, 2 and 10  $\mu\text{g/ml}$  GO coated membranes for 1, 3 and 7 days. The histogram represents Alamar blue reduction percentage in uncoated and GO coated membranes. Data shown are the mean ( $\pm$ SD) of three separate experiments. \* 2  $\mu\text{g/ml}$ , 10  $\mu\text{g/ml}$  GO day 3 vs w/o GO day 3,  $p < 0.01$ .

In order to evaluate the biocompatibility of the membranes coated with GO, LDH cytotoxicity assay was performed. A significantly lower LDH leakage by *HGFs* cultured on both test and control membranes on day 7 with respect to day 3 was shown, while no differences were observed between day 1 and day 3. Also, the presence of GO on the membranes did not affect LDH leakage at any experimental time (Figure 7).

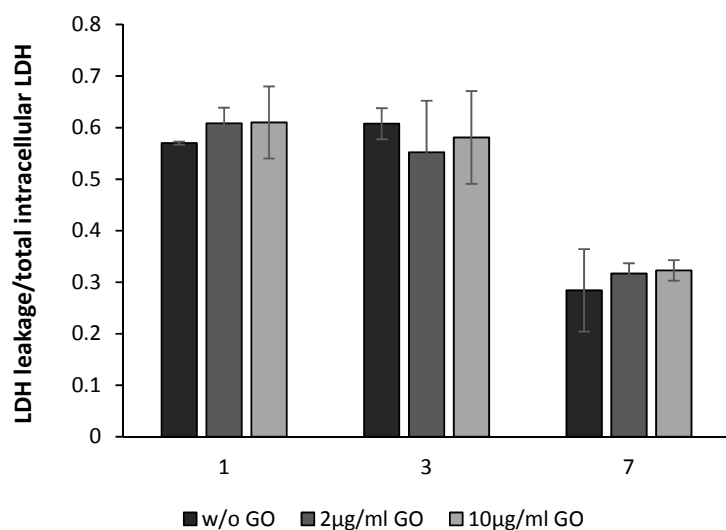


**Figure 7** LDH Cytotoxic assay of *HGFs* cultured on uncoated, 2 and 10 µg/ml GO coated membranes for 1, 3 and 7 days. Values are reported as LDH leakage/total intracellular LDH.

\* w/o GO day 7 vs w/o GO day 1, day 3,  $p < 0.01$ . \* 2 µg/ml GO day 7 vs 2 µg/ml GO day 1, day 3,  $p < 0.01$ . \* 10 µg/ml GO day 7 vs 10 µg/ml GO day 1, day 3,  $p < 0.01$ .

To investigate the occurrence of an inflammatory event, ELISA assay was performed in order to detect IL-6 and PGE2 pro-inflammatory cytokines secretion levels in the culture medium. At day 3 the IL-6 secretion level was significantly lower in cells cultured on membranes coated with both 2 µg/ml and 10 µg/ml GO with respect to those grown on control membranes, while at other experimental times no statistically significant difference was revealed (Figure 8a). The secretion levels of PGE2 at day 1 and day 7 did not show a significant difference between the control membrane and both test membranes, however at day 3 the control membrane showed a significantly higher secretion level than both test membranes. Although secretion levels of PGE2 through time showed a trend to decrease in the presence of all membranes, the only statistically



significant decrease was observed between day 3 and day 7 in cells grown on membranes coated with 2  $\mu\text{g/ml}$  GO (Figure 8b).

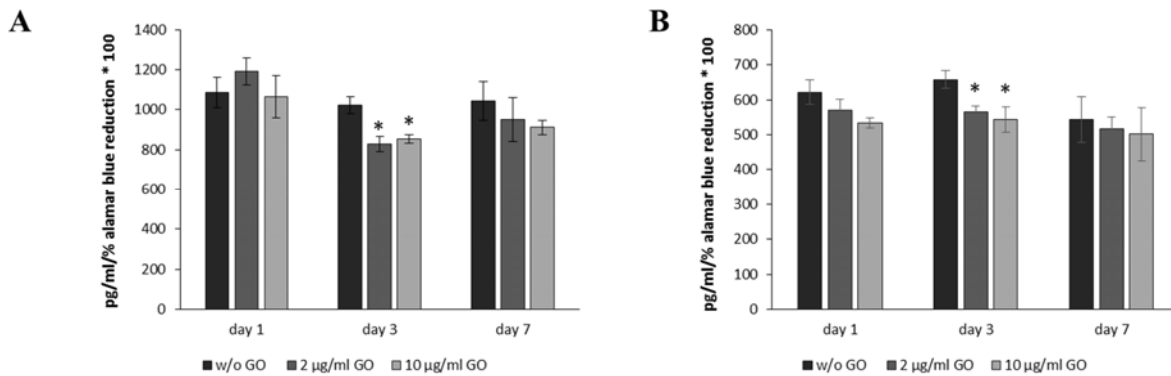


**Figure 8** ELISA assay for IL6 (a) PGE2 (b) secretion of *HGFs* cultured on uncoated, 2 and 10  $\mu\text{g/ml}$  GO coated membranes for 1, 3 and 7 days. Secretion levels are reported as picograms per milliliter/% Alamar blue reduction  $\times 100$ . The results are the mean  $\pm$  SD of three samples from three different experiments. \* 2  $\mu\text{g/ml}$ , 10  $\mu\text{g/ml}$  GO day 3 IL6 secretion level vs w/o GO day 3 IL6 secretion level,  $p < 0.01$ . \* 2  $\mu\text{g/ml}$ , 10  $\mu\text{g/ml}$  GO day 3 PGE2 secretion level vs w/o GO day 3 PGE2 secretion level,  $p < 0.01$ .

#### 4. Discussion

Collagen membranes were easily coated with GO by simply drop casting the aqueous GO solution of proper concentration on the membrane. The GO demonstrated to be well distributed on the surface although AFM analysis evidenced that GO is not forming a continuous film. SEM analyses highlighted the presence of some frustules on the surface of 2  $\mu\text{g/ml}$  GO coated membrane that disappeared in 10  $\mu\text{g/ml}$  GO coated one. An higher concentration of GO rendered the surface apparently more smooth, as already recently evidenced in the case of porcine bone granules [22]. This smoothness is only apparent because the calculated roughness indexes, although relative only

to the imaged samples and therefore characterized by a high error, were  $R_q = 62.8$  nm,  $R_a = 50$  nm, image  $R_{max} 401$  nm,  $Sdq 40.6^\circ$ ,  $Sdr 32.3\%$ . for the bare membrane (See Figure S12 in the Supplementary Data) and  $R_q = 177$  nm and  $R_a = 141$  nm, image  $R_{max} 973$  nm,  $Sdq 45^\circ$ ,  $Sdr 42.4\%$  for the GO-coated sample (See Figure S13 in the Supplementary Data), where  $R_q$  is the roughness least square value;  $R_a$ , the average of the absolute values of the surface high deviations; Image  $R_{max}$ , the maximum vertical distance between the highest and lowest data points in the image following the plane fit;  $Sdq$ , the root-mean-square of the surface slope and  $Sdr$ , the developed interfacial area ratio. In terms of  $R_q$  and  $R_a$ , the non-coated membrane highlighted a lower roughness, as compared to the GO-coated sample, with slightly lower peaks, as confirmed by imaged  $R_{max}$  values. The surface indexes were in agreement with the previous data because  $Sdr$  and  $Sdq$ , that were expected to give the surface enlargement induced by the presence of roughness and an idea of the steepness of the peaks, evidenced more and steeper peaks in the coated sample.

GO-coated membranes have been characterized by Peak Force QNM. Despite adhesion, dissipation energy and deformation maps, reported in Figure 3, evidences the presence of regions with different features on the coated sample (i.e. the upper right corner with the GO flakes and the bottom region), quantification of the obtained data should be performed with caution. Indeed the adhesion force between the tip and the substrate, mainly associated with electrostatic and van der Waals interactions, may be affected by attractive capillary forces especially when we consider that the collagen membrane is partially hydrated (i.e. measures are performed in air and not under controlled anhydrous conditions) [31]. The obtained data highlight that the adhesion of the tip to the surface increases on coating the membrane with GO. In particular, in the same membrane the top right region coated with GO evidences a tip adhesion 2 times higher than that measured in the

bottom region. The higher adhesion of the GO for the tip can be due to electrostatic interactions between the negative surface charge of GO [22] and the tip although an adhesion increase, due the formation of a capillary meniscus, cannot be excluded.

The value of dissipation energy for the bare membrane (i.e.  $120\pm 30$  eV) is in agreement with the value previously measured for a hydrated collagen fiber [32]. Considering that an elastic sample is characterized by low dissipation energy values, the obtained energy dissipation value is indicative of a non perfectly elastic sample (i.e. viscoelastic behavior). In the GO coated membrane the dissipation energy measured for the GO-coated membrane is one third higher than that measured for the pure membrane, dissipation energy being higher on the GO flakes with respect to the bottom region. These data are difficult to explain and probably they may be affected by water bridge formation [32] favored by the establishment of hydrogen bonds among acid, carbonyl and ether groups of GO and water, that hamper a properly measure of the viscoelastic properties. Indeed, the small elastic deformability of GO-coated membranes may be the result of the stiffness conferred to the membrane by GO flakes. Since collagen fibers demonstrated to increase their deformation on increasing hydration [32], the observed decrease of deformation of the GO-coated membrane may be as well imputed to a reduction of collagen hydration due to the preference of collagen to form hydrogen bonds with GO rather than with water.

Stability measurements obtained by membrane immersion in water evidenced no apparent dissolution of graphene oxide in solution after 7 days of contact.

Collagen membranes coated with different GO concentrations were then tested in a human gingival fibroblasts biological model in order to check their early adhesion and proliferation on barrier membranes which switch on a healing process after surgical procedures.

During all the fibroblasts culture period, GO addition did not negatively affect the biological parameters evaluated, thus indicating, at a glance, a good tolerability. In particular, GO coating, both at low and high concentration, enhanced the proliferation rate of fibroblasts and at the same time, it ensured an appreciable control of inflammatory events which appeared less pronounced in coated membranes. As expected, these evidences appeared statistically significant only after three days of culture as the average doubling time of cultured fibroblasts is estimated to be  $33.2 \pm 10.4$  hours in an *in vitro* physiological condition [33]. For this reason after 24 hours of culture, gingival fibroblasts were still starting up their metabolism thus proliferation and secretion events were scarcely appreciable. On the other hand, after 7 days of culture it could be easily expected that the cells reached a confluence condition on the available surface.

These results may be connected with the demonstrated ability of GO to favour protein adsorption [34], an essential step for regulating cell functions and mediate cell adhesion and morphology [35]. This means that the presence of GO should favour cell adhesion and the subsequent cells growth. Analogously, by adsorption of IL-6 and PGE2 pro-inflammatory cytokines, this same effect could affect their quantification in the culture medium. Nevertheless this event seems unlikely because, during pro-inflammatory cytokines quantification, the GO-coated membrane was already covered, and therefore almost saturated, with proteins and cells. These preliminary conclusions paves the way for interesting discussions and further studies on the subject.

## **Conclusions**

This study evidenced that the coating with GO of commercial collagen membranes was relatively homogeneous and easy to obtain. No evidence of release of GO in the aqueous medium was observed in a time interval of 7 days. The presence of GO onto the membrane demonstrated to alter the mechanical features of the membrane conferring a lower deformability, likely connected

with a higher stiffness and reduced hydration, and higher roughness with respect to the bare membrane. These changes demonstrated to favor the proliferation rate of *HGFs*, avoiding to induce an inflammatory response, as checked by ELISA test of both IL6 and PGE2 secretion, probably due to the capacity of GO to adsorb proteins and promote cell adhesion. This study paves the way to the further investigation of this novel coated membranes in terms of promotion of osteoblast differentiation and/or bacteriostatic activity.

### **Acknowledgement**

The Authors thanks the Universities of Chieti-Pescara and MIUR (PRIN 2010-11, prot. 2010N3T9M4 and FIRB 2010, prot. RBAP1095CR) for financial supports.

## References

- [1] P. Bunyaratavej, H.L. Wang, 2001. *J. Periodontol.*, 72: 215-229.
- [2] C.H.F. Hämmerle, R. Jung, 2003. *Periodontology 2000*, 33: 36-53.
- [3] T. Karring, F. Isidor, S. Nyman, J. Lindhe, 1985. *J. Clin. Periodontol.*, 12: 51–60.
- [4] A. K. Schlegel, H. Möhler, F. Busch, A. Mehl, 1997. *Biomaterials*, 18: 535-538.
- [5] P. Locci, M. Calvitti, S. Belcastro, M. Pugliese, M. Guerra, L. Marinucci, N. Staffolani, E. Becchetti, 1997. *J. Periodontol.*, 68: 857-863.
- [6] D. Rothamel, F. Schwarz, A. Sculean, M. Herten, W. Scherbaum, J. Becker, 2004. *Clin. Oral. Implant. Res.*, 15: 443-449.
- [7] G. Brunel, P. Piantoni, F. Elharar, E. Benque, P. Marin, S. Zahedi, 1996., *J. Periodontol.*, 67: 1342–1348.
- [8] S. Pitaru, M. Noff, A. Grosskopf, O. Moses, H. Tal, N. Savion, 1991. *J. Periodontol.*, 62: 598-601.
- [9] A. El-Fiqi.,J.H. Lee, E.J. Lee, H.W. Kim, 2013. *Acta Biomater.*, 9: 9508-9521.
- [10] A. Geim, K. Novoselov, 2007. *Nat. Mater.*, 6: 183-191.
- [11] J.L. Sabourin, D.M. Dabbs, R.A. Yetter, F.L. Dryer, I.A. Aksay, 2009. *ACS Nano*, 3: 3945-3954.
- [12] J. Zhang, H. Yang, G. Shen, P. Cheng, J. Zhang, S. Guo, 2010. *Chem. Commun.*, 46: 1112-1114.
- [13] X. Sun, Z. Liu, K. Welsher, J.T. Robinson, A. Goodwin, S. Zaric, H. Dai, 2008. *Nano Res.*, 1: 203-212.
- [14] W. Zhang, Z. Guo, D. Huang, Z. Liu, X. Guo, H. Zhong, 2011. *Biomaterials*, 32: 8555-8561.
- [15] H. Chen, M.B. Muller, K.J. Gilmore, G.G. Wallace, D. Li, 2008. *Adv. Mater.*, 20: 3557–3561.

- [16] S. Agarwal, X. Zhou, F. Ye, Q. He, G.C. Chen, J. Soo, F. Boey, H. Zhang, P. Chen, 2010. *Langmuir*, 26: 2244–2247.
- [17] E. Nishida, H. Miyaji, A. Kato, H. Takita, T. Iwanaga, T. Momose, K. Ogawa, S. Murakami, T. Sugaya, M. Kawanami, 2016. *Int. J. Nanomed.*, 11: 2265–2277.
- [18] S. Park, N. Mohanty, J.W. Suk, A. Nagaraja, J. An, R.D. Piner, W. Cai, D.R. Dreyer, V. Berry, R.S. Ruoff, 2010. *Adv. Mater.*, 22: 1736–1740.
- [19] A.C. Ferrari, F. Bonaccorso, V. Fal'ko, K.S. Novoselov, S. Roche, P. Bøggild, S. Borini, F.H. L. Koppens, V. Palermo, N. Pugno, J.A. Garrido, R. Sordan, A.o Bianco, L. Ballerini, M. Prato, E. Lidorikis, J. Kivioja, C. Marinelli, T. Ryhänen, A. Morpurgo, J.N. Coleman, V. Nicolosi, L. Colombo, A. Fert, M. Garcia-Hernandez, A. Bachtold, G.F. Schneider, F. Guinea, C. Dekker, M.o Barbone, Z. Sun, C. Galiotis, A.N. Grigorenko, G. Konstantatos, A. Kis, M. Katsnelson, L. Vandersypen, A. Loiseau, V. Morandi, D. Neumaier, E. Treossi, V. Pellegrini, M. Polini, A. Tredicucci, G.M. Williams, B.H. Hong, J.-H. Ahn, J. M. Kim, H. Zirath, B.J. van Wees, H. van der Zant, L. Occhipinti, A. Di Matteo, I.A. Kinloch, T. Seyller, E. Quesnel, X. Feng. K. Teo, N. Rupesinghe, P. Hakonen, S.R.T. Neil, Q. Tannock, T. Löfwanderaq, J. Kinaret, 2015. *Nanoscale* 7: 4598-4810.
- [20] W. Hu, C. Peng, W. Luo, M. Lv, X. Li, D. Li, Q. Huang, C. Fan, 2010. *ACS Nano*, 4: 4317–4323.
- [21] K.H. Liao, Y.S. Lin, C.W. Macosko, C.L. Haynes, 2011. *ACS Appl. Mater. Interfaces*, 3: 2607–2615.
- [22] V. Ettore, P. De Marco, S. Zara, V. Perrotti, A. Scarano, A. Di Crescenzo, M. Petrini, C. Hadad, D. Bosco, B. Zavan, L. Valbonetti, G. Spoto, G. Iezzi, A. Piattelli, A. Cataldi, A. Fontana, 2016. *Carbon*, 103: 291-298.

- [23] W.S. Hummers, R.E. Offeman, 1958. *J. Am. Chem. Soc.*, 80: 1339-1339.
- [24] T. Rattana, S. Chaiyakun, N. Witit-anun, N. Nuntawong, P. Chindaudom, S. Oaew, C. Kedkeaw, P. Limsuwan, 2012. *Procedia Eng.*, 32: 759-764.
- [25] I. Horcas, R. Fernández, J. M. Gómez-Rodríguez, J. Colchero, J. Gómez-Herrero, A. M. Baro, 2007. *Rev. Sci. Instrum.*, 78: 013705.
- [26] M. Radunovic, M. De Colli, P. De Marco, C. Di Nisio, A. Fontana, A. Piattelli, A. Cataldi, S. Zara, submitted to *Journal of Biomedical Materials research, part A*.
- [27] D.-D. Han, Y.-L. Zhang, Y. Liu, Y.-Q. Liu, H.-B. Jiang, B. Han, X.-Y. Fu, H. Ding, H.-L. Xu, H.-B. Sun, 2015. *Adv. Funct. Mater.*; 25: 4548-4557.
- [28] Y.F. Dufrêne, D. Martínez-Martín, I. Medalsy, D. Alsteens. D.J. Müller, 2013. *Nat. Methods*, 10: 847–854
- [29] D. Alsteens, V. Dupres, S. Yunus, J.-P. Latgé, J.J. Heinisch, Y.F. Dufrêne, 2012. *Langmuir*, 28: 16738–16744.
- [30] K.S. Weadock, E.J. Miller, L.D. Bellincampi, J.P. Zawadsky, M.G. Dunn, 1995. *J. Biomedical Mater. Res.*, 29: 1373-1379.
- [31] L. Zitzel, S. Herminghaus, F. Mugele, 2002, *Phys. Rev. B*, 66, 155436.
- [32] M.R. Uhlig, R. Magerle, 2017, *Nanoscale*, 9, 1244-1256.
- [33] T. Mio, S. Nagai, M. Kitaichi, A. Kawatani, T. Izumi, 1992. *Chest*, 102: 832-837.
- [34] W.C. Lee, C.H.Y.X Lim, H. Shi, L.A.L Tang, Y. Wang, C. T. Lim, K. P Loh, 2011. *ACS Nano*, 5: 7334–7341.
- [35] K.M. Woo, V.J. Chen, P.X. Ma, 2003. *J. Biomed. Mater. Res., Part A*, 67A: 531–537.